

Patterns of CO₂ exchange and productivity of the herbaceous vegetation and trees in a humid savanna in western Kenya

Dennis Otieno · Joseph Ondier · Sebastian Arnhold · Daniel Okach ·
Marianne Ruidisch · Bora Lee · Andreas Kolb · John Onyango ·
Bernd Huwe

Received: 9 March 2015 / Accepted: 18 September 2015 / Published online: 23 September 2015
© Springer Science+Business Media Dordrecht 2015

Abstract Factors governing the dynamics between woody and herbaceous vegetation in the savanna are of ecological interest since they determine ecosystem productivity and stability. Field measurements were conducted in a humid savanna in the Lambwe valley, western Kenya, to compare CO₂ exchange of the herbaceous vegetation and trees and its regulation. Soil characteristics and root distribution patterns

under tree canopies and in the open locations dominated by the herbaceous vegetation were profiled in 1-m-deep soil layers. Soil water content (SWC) was measured at 30 cm depth both in the herbaceous vegetation and also under the tree canopies. The mean maximum monthly gross primary production (GPP_{max}) in the herbaceous vegetation was determined from chamber measurements, while daily GPP (GPP_{day}) in both the grass and tree canopies was simulated using the PIXGRO model. The highest mean GPP_{max} in the herbaceous vegetation was $26.2 \pm 3.7 \mu\text{mol m}^{-2} \text{ s}^{-1}$ during April. Seasonal fluctuations of GPP in the herbaceous vegetation were explained by soil water availability ($R^2 = 0.78$) within the upper 30-cm soil profile. Seasonal GPP_{day} fluctuations were larger (between $1 \text{ gC m}^{-2} \text{ d}^{-1}$ and $10 \text{ gC m}^{-2} \text{ d}^{-1}$) in the herbaceous vegetation compared to the trees, which fluctuated around $4.3 \pm 0.3 \text{ gC m}^{-2} \text{ d}^{-1}$ throughout most of the measurement period. Daily tree canopy transpiration (E_c), canopy conductance (G_c), and GPP_{day} were decoupled from SWC in the top 30-cm soil profile. On average, ecosystem GPP_{day} (mean of tree and herbaceous vegetation) was $14.3 \pm 1.2 \text{ gC m}^{-2} \text{ d}^{-1}$ during the wet period and $6.1 \pm 0.9 \text{ gC m}^{-2} \text{ d}^{-1}$ during drought. Differences between the herbaceous and tree canopy responses were attributed to soil moisture availability.

Communicated by T.L. Pons.

Electronic supplementary material The online version of this article (doi:[10.1007/s11258-015-0523-3](https://doi.org/10.1007/s11258-015-0523-3)) contains supplementary material, which is available to authorized users.

D. Otieno (✉) · D. Okach · M. Ruidisch · B. Lee
Department of Plant Ecology, University of Bayreuth,
95440 Bayreuth, Germany
e-mail: denotieno@yahoo.com;
dennis.otieno@uni-bayreuth.de

J. Ondier · J. Onyango
Department of Botany, Maseno University,
P.O. Box 333, Maseno, Kenya

S. Arnhold · A. Kolb · B. Huwe
Department of Soil Physics, University of Bayreuth,
95447 Bayreuth, Germany

S. Arnhold
Professorship of Ecological Services, University of
Bayreuth, 95447 Bayreuth, Germany

Keywords Canopy conductance · Canopy transpiration · Gross primary production · Hydraulic lift · Humid savanna · Soil water availability

Introduction

Savannas are tropical and sub-tropical ecosystems defined by a discontinuous tree canopy matrix above a seasonally continuous herbaceous vegetation that occur naturally in Africa, Australia, Asia, the Americas, and southern parts of Europe (Scholes and Archer 1997). They cover approximately 17×10^6 km² of the Earth's land surface and must play a significant role in the global carbon budget and regional hydrological cycles (Miranda 1997). Factors governing the dynamics between woody and herbaceous vegetation have been of primary interest since they determine ecosystem productivity and stability (Walter 1971; Noy-Meir 1982; Walker and Noy-Meir 1982; Sankaran et al. 2004; Baudena et al. 2010). The two-layer hypothesis by Walter (1971) proposed a compartmentalized soil resource base, whereby trees draw their water supply from the deeper, more stable soil moisture reserves, while roots of the herbaceous vegetation are restricted to the shallow soil layers (Walter 1971; Noy-Meir 1982; Walker and Noy-Meir 1982). Trees, therefore, remain physiologically active for longer, during the development of drought and exhibit higher rates of CO₂ exchange compared to the herbaceous vegetation, due to extended moisture availability in the deeper soil profiles (Scholes and Walker 1993; Scholes and Archer 1997; Jenerette et al. 2008; Scott et al. 2014).

In humid savannas, however, frequent rainfall and high soil moisture availability during most of the year may not support the development of deep rooting systems. Both the trees and the herbaceous vegetation, therefore, rely on water available in the shallow soil layers (Belsky 1994; Mordelet et al. 1993; Le Roux et al. 1995; Eamus et al. 2001) and are likely to demonstrate similar trends of CO₂ fluxes during most of the year, given that in most savannas soil moisture controls most of the ecosystem processes (Walter 1971; Noy-Meir 1982; Frost et al. 1986). Ecophysiological studies in some moist savannas, however, have shown higher leaf gas exchange rates in trees compared to the herbaceous vegetation during the short drought intervals (Myers et al. 1997; O'Grady et al. 1999; Hutley et al. 2000). Such differences may be attributed to (1) facilitation of water infiltration after a rain event by the trees, resulting in higher sub-canopy soil moisture compared to the exposed inter-canopy soils dominated

by the herbaceous vegetation (Devitt and Smith 2002; Bhark and Small 2003); (2) reduced soil evaporation through canopy shading, facilitating sustained high soil moisture availability under tree crowns during the development of drought (Weltzin and Coughenour 1990; D'Odorico et al. 2007); (3) extensive, lateral rooting system and access to soil moisture beyond their crowns in trees (Belsky 1994; Casper et al. 2003; Wang et al. 2007); or/and (4) differential rooting systems between trees and the herbaceous vegetation that allow trees to access more stable, deep water resources (Scott et al. 2006; Jenerette et al. 2008; Barron-Gafford et al. 2012).

While the co-dominance of trees and the herbaceous vegetation in humid savannas in East Africa has evolved under conditions of high soil moisture availability most of the year, the current climate predictions point to a significant decline in rainfall amounts and an increase in air temperatures by 2100 (Cook and Vizy 2013; Dai 2011; Sillmann et al. 2013). Changing precipitation pattern and temperature will potentially alter soil moisture distribution patterns and atmospheric vapor demand, and are likely to change the way these savannas are structured and their functioning as well. As evidenced in a number of savannas and savanna-type ecosystems in Africa and elsewhere, declining ground water table as a result of increasing drought has led to significant woody vegetation encroachment (Archer et al. 2000; Hudak and Wessman 1998; Roques et al. 2001). These studies show that in the event of drought the woody vegetation has a competitive advantage over grasses because they are deep rooted and can take advantage of the deep aquifers during drought, when water resources in the shallow soil layers are depleted (Jenerette et al. 2008; Barron-Gafford et al. 2012; Scott et al. 2014). Such observations are of significant ecological interest, but very poorly understood in the East African humid savannas. Reduced precipitation will alter moisture distribution in the soil substrate, a change that is likely to influence the coupling between plants and their environment, impacting vegetation functioning (Jenerette et al. 2008; Barron-Gafford et al. 2012; Scott et al. 2014; Ahlström et al. 2015) and distribution (Midgley and Thuiller 2010). This calls for better understanding of the linkages between the physical drivers of ecosystem processes, structure, and productivity of the humid savanna in its current state.

A recent study in a humid savanna in the Lambwe valley in western Kenya has demonstrated a strong decline in CO₂ exchange and productivity of the herbaceous vegetation during the dry periods (K'Otuto et al. 2013). For this ecosystem, however, information regarding tree responses is lacking. We still do not understand the functional relationships between the trees and the herbaceous vegetation, which ultimately determine how the ecosystem reacts to changing rainfall regimes. How the two vegetation components relate to seasonal variations in soil moisture resources may provide hints as to how the ecosystem may react to future climate. In this study, we examined soil characteristics, seasonal soil water content (SWC), root distribution patterns, and CO₂ exchange of the herbaceous vegetation and trees of the humid savanna in Lambwe valley. We hypothesized that in this humid savanna, (1) trees improve water infiltration and soil moisture availability within their rhizosphere; (2) trees and the herbaceous vegetation in this humid savanna exhibit different rooting patterns and have access to different soil water resources; and (3) canopy CO₂ exchange in both the trees and the herbaceous vegetation is governed by soil moisture availability.

Materials and methods

Site description

The measurements were conducted in a humid savanna in Ruma, located within the Lambwe valley (00° 35' S & 34° 12' E) in Nyanza Province, Suba District in western Kenya. The altitude of the area is around 1300 m above sea level. The site was located on a north eastern-facing slope at the foothills of the Gwasi massif. The climate is warm and humid, with a mean (2003–2013) annual air temperature of 22 °C. In addition to the expansive savanna with semi-natural vegetation, other land cover types include a conserved area under the Ruma National Park, human settlements, open cattle grazing fields, and seasonally cultivated crop fields (Maitima et al. 2010). The mean annual rainfall (1993–2013) is 1100 mm, with a weak bimodal distribution pattern between April–June and September–November. January–March is usually the driest and hottest period of the year. Soils here are shallow, stony, red-brown clay loams. The higher elevations support ferruginous tropical soils and

halomorphous soils on rocks that are rich in ferromagnesian minerals. Mixed soil formations of red-brown friable clays, gray mottled clays, and gray compacted loamy sands predominate. Down towards the valley bottom, the soils are largely black clays, i.e., “black cotton.” Soils here have a high mineral content and tend to be alkaline (Allsopp and Baldry 1972).

The hills are covered with trees, whose density and diversity decrease down slope where the herbaceous vegetation dominates. Our measurements were conducted on a slightly sloping (slope = 3°), 150 ha terrain mainly rolling grassland, with tracts of open woodland and thickets dominated by tree species of *Acacia*, *Bridelia*, *Combretum*, and *Rhus* (Table 1), and a wide diversity of herbaceous vegetation, dominated by the grass species *Hyparrhenia filipendula* (Table 2). Tree canopy cover at the measurement site was ~20 %. The water table is estimated at 10–15 m, fluctuating between the rainy and dry seasons (communication from the NYS).

Measurements

Microclimate

Between 2008 and 2012, weather parameters were measured with independent sensors that were either connected to a data logger (DL2e, Delta-T Devices, Cambridge, UK) or had standing alone loggers. Precipitation (RG3 HOB0 pedant rain gauge, HOB0ware, Eichstetten, Germany), air humidity and temperature (FUNKY-Clima, ESYS, Berlin, Germany), and soil temperature at –10 and –30 cm (HOB0ware, SynoTech, Linnich, Germany) were measured every 5 min, and data were averaged and logged half-hourly. In Feb 2013, we installed an automatic weather station (AWS- WS-GP1, Delta-T Devices, Cambridge, UK) within the study site to measure and record half-hourly averages of 5-min readings of solar radiation, wind speed and direction, air temperature and humidity, and total rainfall.

Analyses of soil characteristics and plant root distribution

Analyses of soil properties were done in 2012 by Arnhold et al. (2015). Soil profiles (~0.5 × 1 m) down to a depth of consolidated rock material were

Table 1 Tree species within the 100 by 90 cm plot where sap flow measurements were conducted

Tree Species	No of individuals measured for sap flow	Number of erect stems with DBH ranges (cm) n		
		5–10	11–20	21–30
<i>Acacia ancistroclada</i>	3		2	2
<i>Anacardium sp.</i>		4	8	1
<i>Areca digitata</i>			9	4
<i>Bridelia scleroneura</i>	3	35	82	8
<i>Combretum molle</i>	6	16	24	
<i>Gardenia urcelliformis</i>		1	5	
<i>Ozoroa insignis</i>		4	1	2
<i>Piliostigma thonningii</i>		3	4	
<i>Rhus natalensis</i>		1	9	1

Individual trees are organized according to Diameter at breast height (DBH) classes

Table 2 Species composition of the herbaceous vegetation in the open spaces outside the tree canopies

Species	Family	% cover
<i>Aspilia pluriseta</i>	Asteraceae	0.6
<i>Themeda triandra</i>	Poaceae	4.2
<i>Berlaria acanthoides</i>	Acanthaceae	5.2
<i>Chloris gayana</i>	Poaceae	9.8
<i>Hyparrhenia filipendula</i>	Poaceae	66.7
<i>Hypoestes aristata</i>	Acanthaceae	2
<i>Justicia striata</i>	Acanthaceae	8.9
<i>Paspalum vaginatum</i>	Poaceae	0.4
<i>Striga asiatica</i>	Orobanchaceae	1
Others		1.2

The contribution of each individual is represented as %cover

dug within the open locations, outside tree canopies, and also at locations under the tree canopies. Each profile was divided into individual soil horizons and subsequently analyzed for depth distributions of rocks, soil texture, bulk density, saturated hydraulic conductivity, and plant available water capacity, carbon (C) and nitrogen (N) contents, and roots. Rock content was estimated within the profile walls by measuring the size of stones and boulders and the amount of coarse fragments in texture samples. Soil texture was obtained through sieving and laser particle measurements (Mastersizer S MAM 5044, Malvern Instruments, Germany). Bulk density was determined from three replicates per horizon of core samples of 100 cm³ that were dried at 105 °C and subsequently weighed. Total C and N contents were quantified by elemental analysis (NA 1500 Analyzer, Carlo Erba Instruments, Italy). Saturated hydraulic conductivity

was estimated using the ROSETTA pedotransfer model (Schaap et al. 2001) based on the measured soil textural distribution (contents of sand, silt, and clay) and bulk density. Plant available water capacity was obtained from the moisture retention curve function (van Genuchten 1980) as the difference between the water content at field capacity (matric potential of -0.03 MPa) and the water content at the permanent wilting point (matric potential of -1.5 MPa). The required retention parameters and shape coefficients of the retention curve were also estimated using the ROSETTA model as a function of textural distribution and bulk density. Coarse (>2 mm diameter) and fine (<2 mm diameter) root densities for each horizon were determined by counting all roots and dividing the number by the area of the profile wall covered by the associated horizon.

Soil water content

Within the herbaceous vegetation, gravimetric soil water content (SWC) was determined monthly at the locations where CO₂ fluxes were measured. Samples were taken using a 3-cm-diameter corer down to 30 cm. Each sample (layer) was immediately weighed before oven drying at 105 °C for 48 h and reweighing. SWC was determined as the relative change in weight between fresh and dry soil samples. Under the trees, continuous SWC in the upper 30-cm soil layer was monitored using Theta probes (type ML 2X, Delta-T Devices, Cambridge, UK). Data were collected every 30 min, averaged, and logged hourly using a data logger (DL 2e-Delta-T Devices, Cambridge, UK).

CO₂ flux measurements and GPP determination in the herbaceous vegetation

Canopy CO₂ assimilation rates (GPP) of the herbaceous vegetation were determined from the monthly CO₂ flux measurements (net ecosystem CO₂ exchange—NEE and Ecosystem respiration— R_{eco}) with chambers between 2008 and 2010 (K'Otuto et al. 2013) and repeated between 2012 and 2013. Measurements of GPP and R_{eco} in the herbaceous vegetation were conducted each month (consecutive 3 days of measurements) using 40 cm × 40 cm × 54 cm (L × W × H) transparent (for NEE) and opaque (for R_{eco}), climate-controlled chambers (see Otieno et al. 2009 for full chamber description). A set of six plastic frames/collars measuring 39.5 cm by 39.5 cm were randomly inserted 4 cm into the ground in the open locations (at least 10 m away from the nearest tree), a month before the measurements were conducted to enclose an area with herbaceous vegetation measuring 39.5 cm by 39.5 cm for characterizing ecosystem CO₂ exchange. During measurements, CO₂ concentration within the chamber was measured continuously for a period of 2–3 min using an infrared gas analyzer (Li-820, LI-COR, USA), logging average values every 15 s.

Air (at 20 cm above the ground surface) and soil (at –10 cm) temperatures inside and outside of the chambers were monitored during CO₂ measurements, and data were logged at the beginning and end of every round of NEE measurement on each plot. Photosynthetic active radiation (PAR) within the chamber and above the vegetation (canopy) were recorded every 15 s (LI-190, LI-COR, USA). During each monthly measurement series, repeated light and dark chamber measurements were conducted between 08:00 h and 18:00 h. To calculate GPP, R_{eco} was estimated for each NEE observation time by linearly extrapolating between R_{eco} observations. GPP was calculated as

$$\text{GPP} = R_{\text{eco}} + \text{NEE}. \quad (1)$$

Continuous GPP rates during the day were calculated by fitting GPP determined from chamber measurements to a hyperbolic light response model, also known as the Michaelis–Menten or rectangular hyperbola model (Owen et al. 2007), using continuously measured PAR data above the grass canopy.

$$\text{GPP} = \left[\frac{\alpha * \beta * \text{PAR}}{\alpha * \text{PAR} + \beta} \right] + \gamma, \quad (2)$$

where α is the initial slope of the curve and an approximation of the canopy light utilization efficiency (CO₂/photon), β is the maximum GPP of the canopy ($\text{GPP}_{\text{max}} - \mu\text{mol CO}_2 \text{ m}^{-2} \text{ s}^{-1}$), PAR is photosynthetic active radiation ($\mu\text{mol photon m}^{-2} \text{ s}^{-1}$), γ is an estimate of the average ecosystem respiration occurring during the observation period ($\mu\text{mol CO}_2 \text{ m}^{-2} \text{ s}^{-1}$), (α/β) is the radiation required for half maximal uptake rate, and $(\beta + \gamma)$ is the theoretical maximum CO₂ uptake capacity. Since the rectangular hyperbola may saturate very slowly in terms of light, the term $(\alpha\beta * \text{PAR})/(\alpha * \text{PAR} + \beta)$ evaluated at a reasonable level of high light (PAR = 1500 $\mu\text{mol photons m}^{-2} \text{ s}^{-1}$) was used in this study to approximate the potential maximum assimilation GPP_{max} and can be thought of as the average maximum canopy uptake capacity during each observation period, noted here as $(\beta + \gamma)_{1500}$. The parameters $(\beta + \gamma)_{1500}$ (e.g., GPP at PAR = 1500) and γ were estimated for each measurement day.

Mean monthly maximum GPP (mean GPP_{max}) was obtained by averaging monthly GPP_{max} rates recorded over the 5-year period during which the measurements were conducted.

Estimation of daily GPP using PIXGRO model

Model characteristics

Daily gross primary production (GPP) for the trees and the herbaceous vegetation were estimated using the PIXGRO model (see Adiku et al. 2006 for full model description). The model PIXGRO consists of two coupled modules, the canopy flux module PROXEL_{NEE} (PROcess pixel net ecosystem exchange model) and vegetation structure module CGRO. The module PROXEL_{NEE} captures canopy processes such as GPP, R_{eco} , NEE, and transpiration. The simulation of GPP is implemented in module PROXEL_{NEE} using algorithms of Farquhar and Caemmerer (1982), modified by Harley and Tenhunen (1991). CGRO simulates growth and development processes, e.g., leaf area index (LAI). This module was developed for C₃ plants. The C₄ plants, however, are known to have less photorespiration compared to the C₃ due to the CO₂ concentration mechanism of the C₄ cycle (Edwards and Walker, 1983; Taiz and Zeiger 1991). In order to simulate GPP for C₄ grasses, leaf internal CO₂ concentration was set to

3000 $\mu\text{mol mol}^{-1}$ (Ruidisch et al. 2015), thus estimating gas exchange under conditions of CO_2 saturation as is the case with C_4 plants.

The simulated LAI from CGRO is passed to the PROXEL_{NEE} canopy process module, and the computed fixed C fluxes are returned to CGRO, which then simulates growth. Dry matter accumulation rate is simulated from the hourly GPP ($\text{molCO}_2 \text{ m}^{-2} \text{ h}^{-1}$) after conversion to gross carbohydrate production rate, P_g ($\text{gCH}_2\text{O m}^{-2} \text{ h}^{-1}$), and the latter reduced by plant respiration losses (Adiku et al. 2006). The canopy was treated as a single layer. Detailed descriptions of the PIXGRO model algorithms are provided in the supplementary material 1.

Model calibration and parameter setting

The PIXGRO model for trees was calibrated using tree canopy transpiration (E_c , Eq. 6) and canopy conductance (G_c , Eq. 7) data derived from sap flow measurements between May 15 and Nov 12 in 2013. For comparison, similar simulation was performed for the herbaceous vegetation for the same period over which sap flow measurements were conducted. The herbaceous vegetation model was calibrated using 2013 GPP and NEE data derived from the chamber measurements.

Sap flow measurements in trees

Sap flux density J_s ($\text{g m}^{-2} \text{ s}^{-1}$) was measured in at least 3 individuals of the three dominant tree species (80 % of crown cover), *Combretum molle*, *Bridelia scleroneura*, and *Acacia ancistroclada* (see Table 1), using custom-made, heat dissipation probes constructed following Granier's (1987) original design. Each sensor consisted of a pair of 2-mm-diameter probes vertically aligned ca. 10 cm apart. Each probe contained an in-built 0.2-mm-diameter copper–constantan thermocouple (see Otieno et al. 2014 for more details on sensor installation and operation). Temperature differences (ΔT °C) between the probes were measured every 10 s, and a 30-min mean value was logged using Delta-T data logger (DL2e, Delta-T Devices, England).

J_s for each sensor was calculated from ΔT in accordance with Granier (1987), assuming zero J_s (i.e., ΔT_{max}) at night and VPD near zero:

$$J_s = 119K^{1.231}, \quad (3)$$

where

$$K = \frac{(\Delta T_{\text{max}} - \Delta T)}{\Delta T}. \quad (4)$$

Tree water use (TWU, kg h^{-1}) was obtained by multiplying J_s by sapwood cross-sectional area (S_A , m^2).

$$TMU = J_{s_i} \cdot S_{A_i}, \quad (5)$$

where J_{s_i} is J_s of the annulus i ($\text{g m}^{-2} \text{ s}^{-1}$) and S_{A_i} is sapwood area of the annulus i (m^2).

In order to calculate canopy transpiration, the trees were grouped into diameter at breast height (DBH, approx 1.5 m height above the ground surface) classes of 0–10, 11–20, and 21–30 cm. Canopy transpiration was calculated for each diameter class by combining mean SFD for each DBH class and total S_A in each DBH class per unit ground area (G_A) (Ewers et al. 2002).

$$E_c = J_s S_A / G_A \quad (6)$$

Canopy conductance (G_c , mm s^{-1}) was determined from E_c rates as

$$G_c = k \frac{E_c}{\text{VPD}} \quad \text{where } k = G_v T_k, \quad (7)$$

where G_v is the universal gas constant = 0.462 $\text{m}^3 \text{ kPa kg}^{-1} \text{ K}^{-1}$) and T_k is the air temperature in Kelvin (K).

Data analysis

Statistical analysis was carried out using the SPSS package. Homogeneity of data from the six different CO_2 measurement soil frames and also soil data from the replicate plots was tested using Shapiro–Wilk test. Soil data from the two locations were compared using t test, at the 5 % level of significance. Factor effects were assessed through regression analyses.

Results

Soil characteristics and root distribution patterns

The depth of soils on which our plots were established ranged between 50 and 70 cm, below which there was

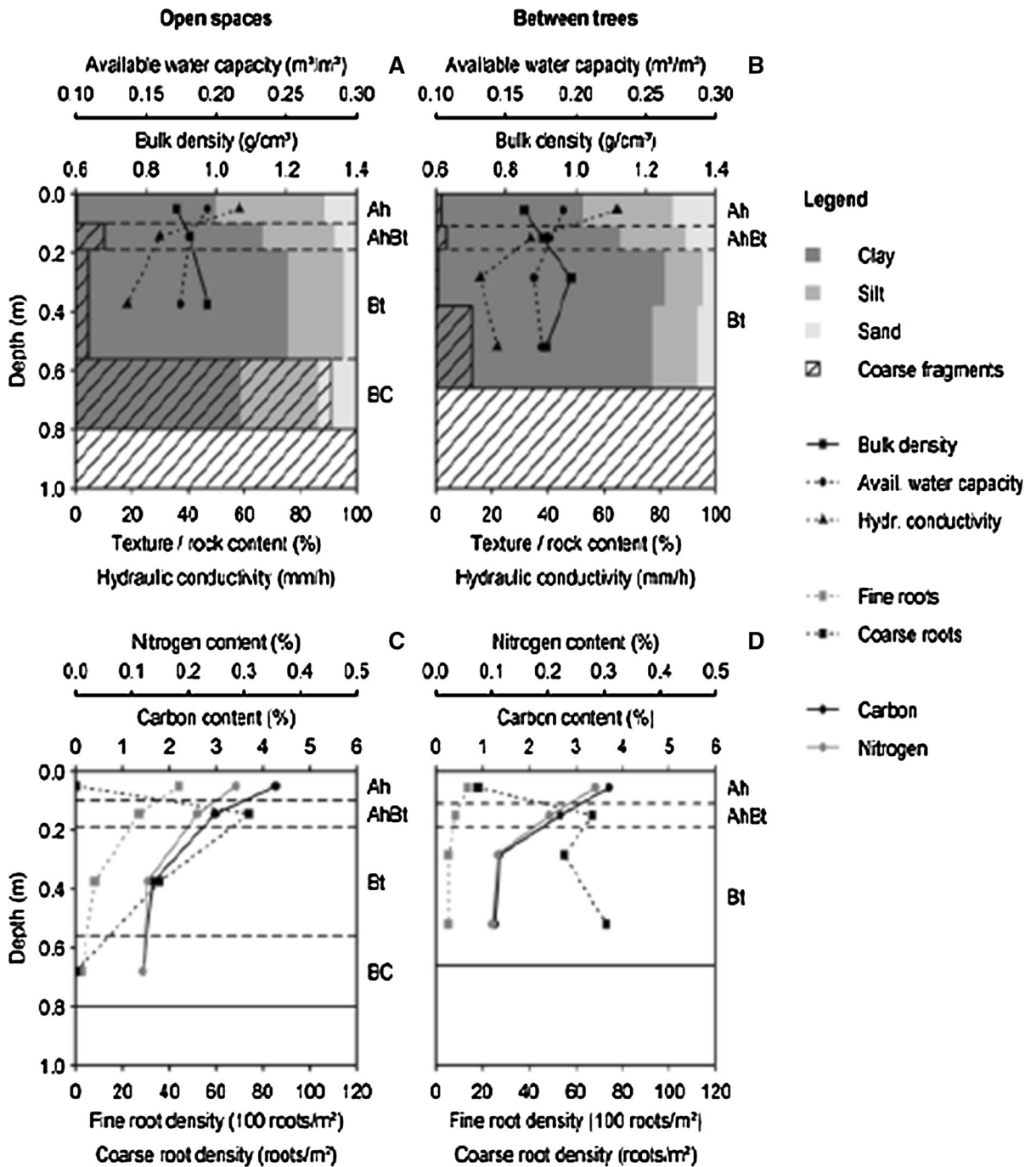


Fig. 1 Soil characteristics including (*upper panel*) soil texture, structure, and hydraulic parameters, (*lower panel*) soil nitrogen and carbon contents, and root distribution in the (a and c)

locations outside the tree canopies dominated by the herbaceous vegetation and (b and d) locations under the tree canopies

a strong presence of coarse rock fragments (Fig. 1a, b). The soil textural composition was 50–80 % clay, 10–40 % silt, and 5–10 % sand, with no differences

between the open locations, outside the tree canopies, and under the tree canopies. In both locations, soil bulk density ranged from 0.8 to 1.0 g cm⁻³, while soil

hydraulic conductivity ranged from 20 to 70 mm h⁻¹. Differences between locations under the tree canopies and the open locations were not significant. Under the tree canopies and in the open locations, soil hydraulic conductivity dropped sharply within the shallow 30-cm soil profile, while plant available water capacity was stable between 0.17 and 0.19 m³ m⁻³. Differences in soil bulk densities and hydraulic properties between the two locations were also not significant. The distribution patterns and quantities of soil C and N within the upper 60 cm of the soil profiles below and outside the tree canopies were similar, with values ranging from 0.3 and 4 % within the top 10-cm soil profile and around 0.1 and 1.5 % in the 40 cm depth for N and C, respectively (Fig. 1c, d).

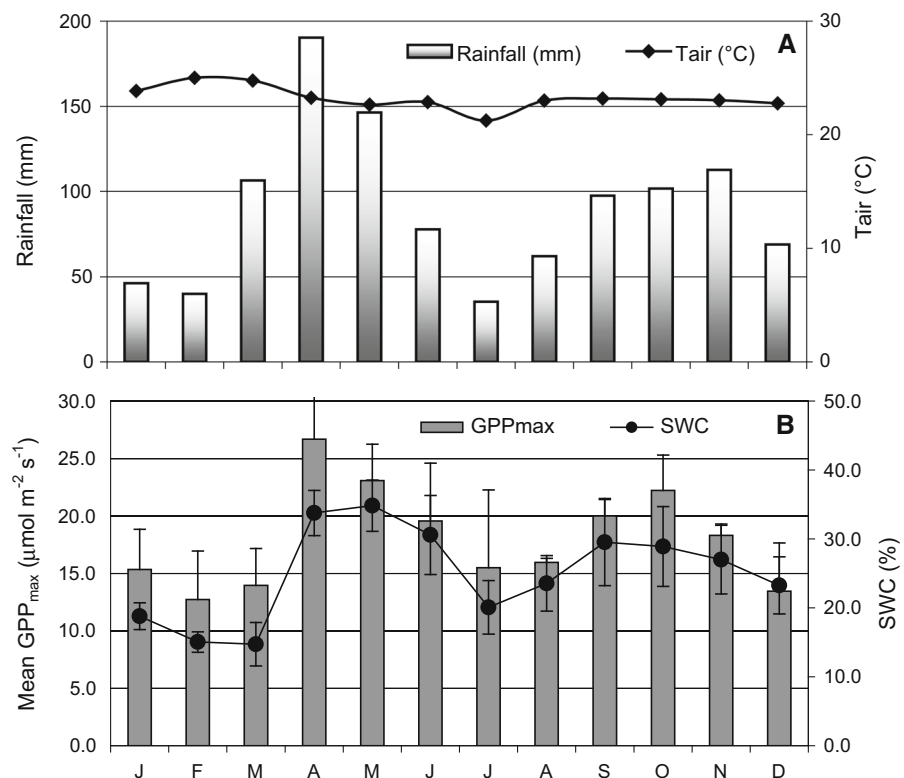
Root distribution patterns were different between the two locations (Fig. 1c, d). In the open locations, the densities of coarse and fine roots were the highest at around 20 cm depth, but declined sharply between 30 and 60 cm depths. Some of the coarse roots found here belonged to the trees, while majority of the fine roots were grass roots. Under the tree canopies, there was a strong increase in coarse root density in the

deeper soils >40 cm depth, all of which belonged to the trees. Fine root density within the top 60-cm soil profile under the tree canopies was low and declined between 10 and 50 cm depths. There was a mix of both trees and grass roots.

Microclimate of the study site

The average monthly air temperatures and total rainfall between 2008 and 2013 during the period of CO₂ measurements in the herbaceous vegetation are shown in Fig. 2. On average, monthly air temperature was 22.3 ± 4 °C, the hottest months being February and March, while the coldest month was July. Daily temperature fluctuations ranged between 12 and 15 °C. Rainfall was bimodal, occurring from mid-March to end of May and from September to November. The average annual precipitation was 1086 ± 230 mm (5-year period). Continuous PAR measurements were only available from Feb 2013, otherwise point measurements were conducted alongside CO₂ flux measurements with the chamber.

Fig. 2 **a** Mean monthly air temperatures (T_{air}) and total monthly rainfall amounts recorded over a period of 10 years between 2004 and 2013 at three climate stations located at different locations around the Ruma National Park. **b** Mean maximum canopy assimilation (A_{max}) and soil water content (SWC) in the herbaceous vegetation between 2008 and 2010 and repeated between May 2012 and December 2013. Bars are standard deviation



Between Feb and Nov 2013, daily sums of PAR ranged between 20 and 49 mol m⁻² d⁻¹.

Canopy gross primary production of the herbaceous vegetation

Canopy GPP of the herbaceous vegetation was higher during the rainy compared to the dry periods (Fig. 2b). Peak instantaneous GPP_{max} rates were 26.2 ± 3.7 μmol m⁻² s⁻¹ recorded in April, while the lowest rates averaged 12.4 ± 4.3 μmol m⁻² s⁻¹ in February, corresponding to the wettest and driest months of the year, respectively (Fig. 2a). A second peak, but lower than that in April, occurred in October, associated with the short rain events. Similar trends were observed for ecosystem respiration (R_{eco}) and net ecosystem CO₂ exchange NEE (See supplementary material 2). SWC at 30 cm depth explained most (R² = 0.78) of the observed variations in GPP_{max} in the herbaceous vegetation (Fig. 3).

Tree canopy transpiration and canopy conductance

Daily transpiration rates, prevailing microclimate, and soil moisture conditions within the upper 30-cm soil layer between March and November 2013 when sap flow measurements were conducted are shown in Fig. 4. The average daily TWU between May and October was ca. 22.4 ± 8.6 kg d⁻¹, contributing to mean daily maximum canopy transpiration (E_c) rates of 1.2 ± 0.1 mm d⁻¹. The highest E_c occurred in June

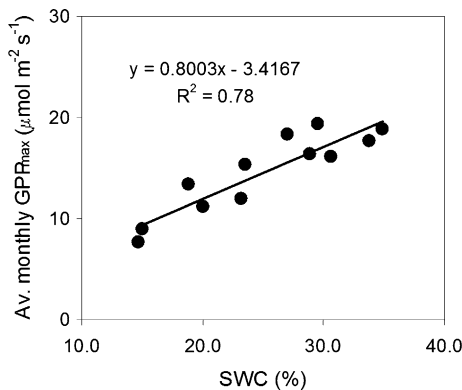


Fig. 3 Response of the average monthly maximum gross primary productivity (GPP_{max}) rates to changing soil water content (SWC) in 30-cm soil profile in the herbaceous vegetation. Data are 3-day records for each month averaged over the period between 2008–2010 and 2012–2013

and in October, associated with the highest canopy conductance (G_c) of around 11.5 mm s⁻¹, while the lowest E_c and G_c rates of 0.7 mm d⁻¹ and 6.2 mm s⁻¹, respectively, occurred between July and September (Fig. 4a). Transpiration remained relatively stable during the measurement period, with slight increase at higher VPD (Fig. 4a, b). There was no relationship between SWC at 30 cm depth and E_c or G_c. Both E_c and G_c were however correlated (R² = 0.62 and 0.50, respectively) with VPD (Fig. 5). While canopy transpiration tended to saturate at higher VPD, G_c was linearly and negatively correlated with VPD.

Simulated daily herbaceous and tree GPP

Simulated daily GPP for the herbaceous and tree canopies between February and September, covering a dry period and a wet period in 2013, are shown in Fig. 6. This was the period when data required for the

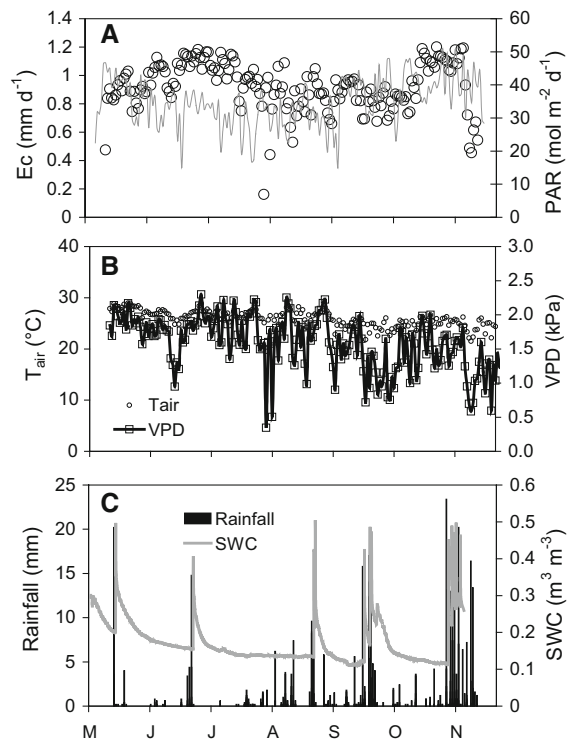


Fig. 4 a Daily tree canopy transpiration (E_c), b mean daily air temperature (T_{air}) and maximum vapor pressure deficit (VPD), and c daily total precipitation and mean soil water content (SWC) within the top 30 cm under the tree canopies between May and November 2013 when sap flow measurements were conducted

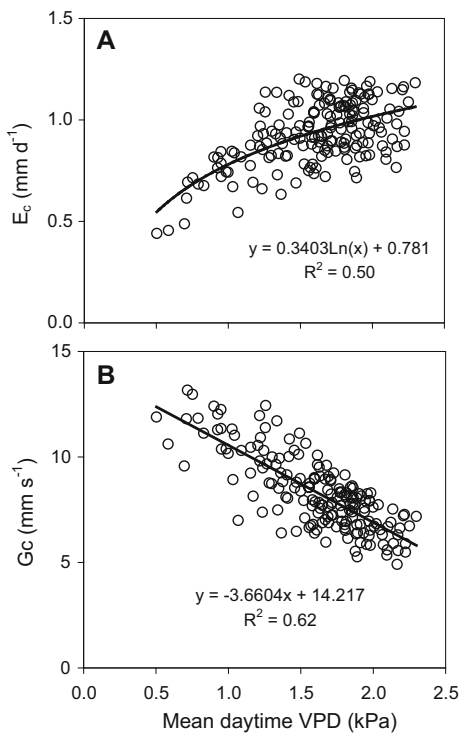


Fig. 5 **a** Response of tree canopy transpiration (E_c) and **b** canopy conductance (G_c) to changes in vapor pressure deficit (VPD) during the day

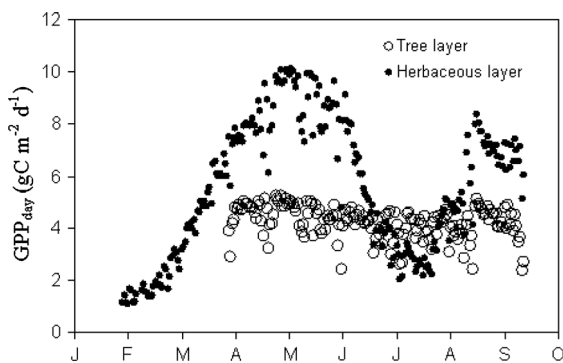


Fig. 6 Simulated daily gross primary production (GPP) of the herbaceous and tree canopies between May and September 2013 when sap flow measurements were conducted

model calibration were available. The highest daily GPP in the herbaceous vegetation occurred between April and May. A second minor peak occurred in September, corresponding to the pattern of monthly GPP_{max} directly measured with the chambers.

Seasonal fluctuations in daily GPP in the herbaceous vegetation were larger compared to trees. The

herbaceous layer GPP rose from $1 \text{ gC m}^{-2} \text{ d}^{-1}$ in February to its peak of $10.2 \pm 0.7 \text{ gC m}^{-2} \text{ d}^{-1}$ in May. A strong decline occurred between June and August, attaining the second lowest daily GPP of $3.4 \pm 1.1 \text{ gC m}^{-2} \text{ d}^{-1}$ during the year. After the September rainfall, there was an increase to a second peak of $7.0 \pm 0.6 \text{ gC m}^{-2} \text{ d}^{-1}$. Unlike the herbaceous vegetation, daily GPP in the tree canopy remained relatively stable at $4.3 \pm 0.3 \text{ gC m}^{-2} \text{ d}^{-1}$, showing less response to SWC within the top 30-cm soil profile. During the rainy periods, tree canopy GPP rates were two times lower than in the herbaceous vegetation. During the dry periods, however, the herbaceous vegetation daily GPP dropped to lower rates compared to the trees. On a ground area basis, the average ecosystem GPP was $14.0 \pm 1.2 \text{ gC m}^{-2} \text{ d}^{-1}$ during the wet periods and dropped to $6.1 \pm 0.9 \text{ gC m}^{-2} \text{ d}^{-1}$ during drought.

Discussion

There was no indication that trees improve soil characteristics related to water infiltration and moisture storage, since particle size distribution, soil organic matter content, soil bulk density, hydraulic conductivity, and available water capacity under the trees and in the open locations dominated by the herbaceous vegetation were similar, disqualifying our first hypothesis (Fig. 1). This was contrary to the previous observations by Belsky et al. (1993) for a semi-arid Kenyan savanna receiving 450 mm rainfall annually. However, like in our case, Hamerlynck et al. (2011) reported lack of influence of trees on soil properties in a semi-arid region with mean annual rainfall of 377 mm. In a study in the Kalahari transect in southern Africa, with rainfall amounts ranging from 365 mm on the driest to 698 mm on the wettest end of the transect, D'Odorico et al. (2007) showed that trees had a positive influence on soil moisture in the dry soils, but this effect was weaker or even neutral in wetter soils. They showed that trees in dry soils improved soil water availability under their canopies by reducing evaporation from the soil surface and by funneling water from their crowns into the soil as stem flow. A similar analysis by Caylor et al. (2005) demonstrated that the influence of trees on soil moisture distribution across the landscape was dependent on the mean annual precipitation. Tree effects on

Table 3 Abbreviations, their descriptions, and units as used in the text

Symbol	Description	Units
Herbaceous vegetation		
GPP_{day}	Gross primary production	$gC\ m^{-2}\ d^{-1}$
GPP_{max}	Maximum gross primary production	$\mu mol\ CO_2\ m^{-2}\ s^{-1}$
R_{eco}	Ecosystem respiration	$\mu mol\ CO_2\ m^{-2}\ s^{-1}$
NEE	Net ecosystem CO_2 exchange	$\mu mol\ CO_2\ m^{-2}\ s^{-1}$
α	Canopy light utilization efficiency	$\mu mol\ CO_2/\mu mol\ photon$
β	Maximum GPP (GPP_{max}) of the canopy	$\mu mol\ CO_2\ m^{-2}\ s^{-1}$
γ	Average ecosystem respiration	$\mu mol\ CO_2\ m^{-2}\ s^{-1}$
$(\beta + \gamma)_{1500}$	Maximum gross primary production	$\mu mol\ CO_2\ m^{-2}\ s^{-1}$
LAI	Leaf area index	$m^2\ m^{-2}$
Trees		
P_g	Gross photosynthesis	$gCH_2O\ m^{-2}\ h^{-1}$
P_{net}	Net photosynthesis	$C\ \mu mol\ m^{-2}\ s^{-1}$
G_v	Gas constant	$kPa\ kg^{-1}\ K^{-1}$
G_A	Ground area	m^2
J_s	Sap flux density	$g\ m^{-2}\ s^{-1}$
S_A	Sapwood area	m^2
DBH	Diameter at breast height	cm
TWU	Tree water use	$kg\ h^{-1}$
G_c	Canopy conductance	
E_c	Canopy transpiration	$mm\ d^{-1}$
Microclimate and soil		
SWC	Soil water content	% volume
VPD	Vapor pressure deficit	kPa
PAR	Photosynthetic active radiation	$\mu mol\ photons\ m^{-2}\ s^{-1}$
T_k	Temperature in Kelvin	K

soil water availability were the strongest at moderate annual precipitation of around 400–500 mm, but disappeared as the mean annual rainfall increased or decreased from this range. While these findings support previous observations and ours too, they did not demonstrate the mechanisms by which trees make soil moisture more available under their canopies. D’Odorico et al. (2007) proposed improved soil water infiltration in dry clayey soils and reduction of evaporative losses by the crown in dry sandy soils as some of the mechanisms through which the positive effects of trees can be attained. Here, we demonstrate that at annual rainfall amounts of around 1100 mm, with soils that are predominantly clay, trees show no significant influence on soil properties related to rain water infiltration and water storage. The only observable difference between locations under the trees and those in the inter-canopy areas, dominated by the herbaceous vegetation, was plant rooting patterns

(Fig. 1), partially supporting our second hypothesis. Thus in our case, differences in the functioning of the herbaceous and tree canopies related to soil moisture availability can only be attributed to rooting patterns of the two vegetation types.

Roots of the herbaceous vegetation were confined to the shallow 60-cm soil profile, while tree roots occurred both in the shallow and deep (> 60 cm depth) soils (Fig. 1c, d). Trees also extended their roots into the open locations outside their crowns. This rooting pattern potentially improves access to soil moisture resources and water uptake by trees compared to the herbaceous vegetation, especially during drought (Belsky et al. 1989; Gibbens and Lenz 2001; Hamerlynck et al. 2011). The presence of tree roots within the shallow soil profiles was also an indication that both trees and the herbaceous vegetation compete for resources, including nutrients and water, as observed in other humid savannas elsewhere (Le

Roux et al. 1995; Eamus et al. 2001). These differences in the rooting patterns between the trees and the herbaceous vegetation likely influence the way the two vegetation types function, including CO₂ exchange and productivity.

Soil moisture in the top 30-cm soil profile explained most ($R^2 = 0.78$) of the observed seasonal fluctuations in CO₂ assimilation rates in the herbaceous vegetation (Fig. 3). This observation agreed with the root distribution data, which showed that most roots of the herbaceous vegetation were confined to the upper 30-cm soil profile (Fig. 1c). Thus the maximum GPP rates (GPP_{\max}) of $26.2 \pm 3.7 \mu\text{mol m}^{-2} \text{s}^{-1}$, recorded in the herbaceous vegetation, coincided with the wet period with highest SWC in the shallow soil layers, while the lowest rates of $13 \pm 3.4 \mu\text{mol m}^{-2} \text{s}^{-1}$ occurred during drought, with the least SWC in the top soil layers. In an arid savanna in South Africa, Kutsch et al. (2008) reported maximum ecosystem GPP rates of $22 \mu\text{mol m}^{-2} \text{s}^{-1}$. Similarly, in an arid Kalahari savanna, with a mean annual precipitation of 365–407 mm, the maximum ecosystem GPP ranged between 15.0 and $20.0 \mu\text{mol m}^{-2} \text{s}^{-1}$. A similar range was reported for a savanna in Botswana receiving 400–464 mm pa (Veenendaal et al. 2004; Williams and Albertson 2004). In a semi-arid Sudanian savanna, canopy assimilation was 16.0 and $2.0 \mu\text{mol m}^{-2} \text{s}^{-1}$ during the wet and dry periods, respectively (Ardö et al. 2008). Thus our GPP_{\max} rates (mean between herbaceous and trees) of around $32 \mu\text{mol m}^{-2} \text{s}^{-1}$ recorded at our site, with an annual rainfall of 900–1300 mm, was realistic. Unlike in most arid savannas where canopy productivity drops to near zero during the dry periods (Ardö et al. 2008; Kutsch et al. 2008), in our case the herbaceous vegetation remained photosynthetically active even during drought, with peak assimilation rates of around $12 \mu\text{mol m}^{-2} \text{s}^{-1}$. Thus, despite periods without rainfall, soil moisture in this savanna remains above a threshold that can support high productivity in the herbaceous vegetation.

The highest mean tree E_c rates were around $1.2 \pm 0.1 \text{ mm d}^{-1}$ but dropped by a small margin to around 0.8 mm d^{-1} during the dry spell. There was no correlation between tree E_c and SWC at 30 cm depth, suggesting that water availability in this soil profile had less influence on tree E_c . This was likely because trees obtain water from soil layers deeper than 30 cm, as demonstrated by the root distribution patterns

shown in Fig. 1d. O’Grady et al. (1999) and Myers et al. (1997) reported lack of differences in tree water use between the wet and dry seasons since trees maintained root–shoot water transport throughout the year in a humid savanna. This was possible because of root access to stable water sources in the deep soils. In a similar humid savanna, Cook et al. (1998) reported that water stored within the 6-m soil profile adequately met tree water requirements during the dry season. These observations are similar to our own, where the trees maintained relatively constant transpiration rates, both during the rainy and dry periods (Fig. 4a). We can confidently conclude that the presence of tree roots in the deeper (>30 cm) soil profiles was responsible for continued high transpiration rates even during drought.

Daily tree E_c increased at higher VPD, but tended to saturate at VPD >1.9 kPa (Fig. 5a), and thus, in many cases, the maximum E_c occurred during the periods when VPD was the highest (Fig. 4a, b). Trees, however, can only transport a given amount of water in their conducting vessels, and hence E_c tends to saturate at higher VPD (Fig. 5a). Excess demand on the water transport apparatus, above the vessel capacity, leads to cavitation unless checked through stomatal closure (Otieno et al. 2007), or by lowering canopy leaf area (Hutley et al. 2000). In our case, trees closed their stomata, leading to a strong reduction in G_c at high VPD values (Fig. 5b). At low VPD (~ 0.5 kPa), the maximum G_c recorded was 12.5 mm s^{-1} , but this declined to around 5 mm s^{-1} at VPD of >2.0 kPa, while E_c remained relatively unchanged, suggesting that water supply to the canopy was less interrupted. In a relatively dry South African savanna, with lower SWC compared to our site, Kutsch et al. (2008) reported a maximum G_c of 9.8 mm s^{-1} during the wet season, but the rates declined to near zero during drought due to lack of soil water. In a semi-arid riparian mesquite woodland in south eastern Arizona, woody vegetation maintained high transpiration rates during summer drought due to access to groundwater (Scott et al. 2006; Barron-Gafford et al. 2012). While G_c declined from 15 to 3 mm s^{-1} in a *Quercus* plantation in a savanna type, Mediterranean ecosystem E_c remained relatively unchanged because of access to groundwater (David et al. 2007).

Changes in G_c due to stomatal response to environmental conditions have implications on

canopy CO₂ uptake, since photosynthesis is coupled to stomatal conductance (Wong et al. 1979; Xu and Baldocchi 2003). For a given amount of water lost, plants maximize the amount of carbon assimilated, leading to an optimal variation in GPP and E_c in space and time (Cowan and Farquhar 1977; Cowan 2002). Thus daily cumulative GPP (GPP_{day}) in the trees remained stable around $4.3 \pm 0.3 \text{ gC m}^{-2} \text{ d}^{-1}$ during the drought despite significant drop in G_c .

A comparison of simulated GPP between the herbaceous and tree canopies showed varying trends and magnitudes between them during the year (Fig. 6). The maximum daily GPP in the herbaceous vegetation was $10.2 \pm 0.7 \text{ gC m}^{-2} \text{ d}^{-1}$ in the wet period compared to $4.3 \pm 0.3 \text{ gC m}^{-2} \text{ d}^{-1}$ estimated for the tree canopy. Daily GPP, however, dropped to $2.1 \pm 1.3 \text{ gC m}^{-2} \text{ d}^{-1}$ in the herbaceous vegetation due to drought stress, while changes in the tree canopy were minimal. Our observations resemble those reported from similar ecosystems elsewhere. In a riparian conservation area in southeastern Arizona, Scott et al. (2014), Barron-Gafford et al. (2012), Jenerette et al. (2008), and Huxman et al. (2004) observed that the C₄ grasses physiologically outperformed the C₃ mesquite woody vegetation during the wet monsoon periods, but were less productive during drought. Differences between the two vegetation types were related to rooting depths, with the woody vegetation having unrestricted access to ground water throughout the year. In an Australian savanna, grasses exhibited 70 % higher daytime GPP compared to the trees during the wet period, but it was 90 % lower during drought. Differences between grasses and trees were attributed to access to deep aquifers by the trees and the loss of C₄-dominated herbaceous vegetation due to drought (Eamus et al. 2001). Compared to most studies reported here, which are from more arid savannas (also see Veenendaal et al. 2004; Williams et al. 2007; Ardö et al. 2008; Kutsch et al. 2008; Merbold et al. 2009; Williams et al. 2009 for African savannas), the period when the herbaceous vegetation maintained higher GPP rates than the trees, during the year, was longer in our case. We attribute this to (1) high rainfall amounts most of the year, hence soil moisture remains relatively above the threshold that supports high productivity; (2) the herbaceous vegetation was dominated by C₄ grasses, which are known to carry out relatively high rates of photosynthesis

under high temperature and conditions that elicit stomatal closure (Caylor et al. 2005); and (3) moderate grazing intensity which allowed for biomass recovery, but at the same time removing the dead aboveground biomass (K'Otuto et al. 2013). The large decline in daily GPP_{day} (Fig. 6) compared to GPP_{max} (Fig. 2) in the herbaceous vegetation during drought is because peak canopy assimilation rates in the herbaceous vegetation occurred during early hours of the day, while the rest of the day was characterized by low CO₂ exchange rates (K'Otuto et al. 2013), contributing to low cumulative GPP. This behavior, combined with the relatively constant E_c rates in the tree canopy during the drought, makes us speculate that hydraulic lift by the tree roots may contribute to the high assimilation rates reported in the herbaceous vegetation during drought. The form of soil moisture measurements conducted in this study, however, was not adequate to confirm this. Due to the high evaporative demand (Fig. 4b), most of the hydraulically lifted water is likely to be rapidly exhausted during the early part of the day. We recommend further investigations in this direction to improve our understanding of the functioning of this savanna.

Conclusions

We made the first attempt to simultaneously assess soil characteristics and root distribution patterns and link them to the productivity of both the herbaceous and woody vegetation in this humid savanna. Our results showed strong variations in rooting patterns between the trees and the herbaceous vegetation. Trees did not show any influence on the soil characteristics related to improved rainwater infiltration or storage. Soil moisture available within the top 30-cm soil profile accounted for most of the herbaceous vegetation GPP, while daily tree canopy GPP and E_c were independent of soil moisture from this layer. The differences between trees and the herbaceous vegetation in their seasonal GPP were linked to their rooting patterns (Fig. 1), which likely access varying moisture sources. Apart from the low grazing intensity and C₄ dominance, we speculate that hydraulic lift by tree roots may contribute to the relatively high GPP_{day} observed in the herbaceous vegetation during drought.

Acknowledgments We thank the Kenya National Youth Service (NYS) Lambwe unit for allowing us to conduct the experiments on their land, for working tirelessly to secure the equipment, and for supporting with data collection. We thank Mrs. Margarete Wartinger for her support with sample analyses. We are grateful to the British Ecological Society (BES) for providing funds for field work under Grant Number: BES 1430-4399.

Compliance with ethical standards

Conflict of Interest The authors declare that they have no conflict of interest.

References

- Adiku S, Reichstein M, Lohila A, Dinh NQ, Aurela M, Laurila T, Lueers J, Tenhunen JD (2006) PIXGRO: a model for simulating the ecosystem CO₂ exchange and growth of spring barley. *Ecol Models* 190:260–276
- Ahlström A, Xia J, Arneeth A, Luo Y, Smith B (2015) Importance of vegetation dynamics for future terrestrial carbon cycling. *Environ Res Lett* 10:054019. doi:10.1088/1748-9326/10/5/054019
- Allsopp R, Baldry DAT (1972) A general description of the Lambwe Valley area of South Nyanza District, Kenya. *Bull World Health Organ* 47:691–697
- Archer S, Boutton-Thomas W, Hibbard KA (2000) Trees in grasslands: biogeochemical consequences of woody plant expansion. In: Schulze E-D, Harrison SP, Heimann M, Holland EA, Lloyd J, Prentice IC, Schimel D (eds) *Global biogeochemical cycles in the climate system*. Academic Press, San Diego
- Ardö J, Mölder M, El-Tahir BA, Elkhidir HAM (2008) Seasonal variation of carbon fluxes in a sparse savanna in semi arid Sudan. *Carbon Balance Manag* 3:7. doi:10.1186/1750-0680-3-7
- Arnhold S, Otieno D, Onyango J, Koellner T, Huwe B, Tenhunen J (2015) Soil properties along a gradient from hill slopes to the savanna plains in the Lambwe Valley, Kenya. *Soil Tillage Res* 154:75–83
- Barron-Gafford GA, Scott RL, Jenerette GD, Hamerlynck E, Huxman TE (2012) Temperature and precipitation controls over leaf- and ecosystem-level CO₂ flux along a woody plant encroachment gradient. *Glob Change Biol* 18:1389–1400
- Baudena M, D'Andrea F, Provenzale A (2010) An idealized model for tree–grass coexistence in savannas: the role of life stage, structure and fire disturbances. *J Ecol* 98:74–80
- Belsky AJ (1994) Influences of trees on savanna productivity: tests of shade, nutrients, and tree-grass competition. *Ecology* 75:922–932
- Belsky AJ, Amundson RG, Duxbury JM, Riha SJ, Ali AR, Mwonga SM (1989) The effect of trees on their physical, chemical, and biological environments in a semi-arid savanna in Kenya. *J Appl Ecol* 6:1005–1024
- Belsky AJ, Mwonga SM, Duxbury JM (1993) Effects of widely spaced trees and livestock grazing on understory environments in tropical savannas. *Agrorfor Syst* 24:1–20
- Bhark EW, Small EE (2003) Association between plant canopies and the spatial patterns of infiltration in shrubland and grassland of the Chihuahuan Desert, New Mexico. *Ecosystems* 6:185–196
- Casper BB, Schenk HJ, Jackson RB (2003) Defining a plant's belowground zone of influence. *Ecology* 84:2113–2321
- Caylor KK, Shugart HH, Rodriguez-Iturbe I (2005) Tree canopy effects on simulated water stress in Southern African savannas. *Ecosystems* 8:17–32. doi:10.1007/s10021-004-0027-9
- Cook KH, Vizzy EK (2013) Projected changes in East African rainy seasons. *J Clim*. doi:10.1175/JCLI-D-12-00455.1
- Cook PG, Hatton TJ, Pidsley D, Herczeg AL, Held A, O'Grady A, Eamus D (1998) Water balance of a tropical woodland ecosystem, Northern Australia: a combination of micro-meteorological, soil physical and groundwater chemical approaches. *J Hydrol* 210:61–177
- Cowan I (2002) Fit, fitter, fittest; where does optimisation fit in? *Silva Fenn* 36:745
- Cowan I, Farquhar G (1977) Stomatal function in relation to leaf metabolism and environment. *Symp Soc Exp Biol* 31:471–505
- Dai A (2011) Drought under global warming: a review. *WIREs Clim Change* 2:45–65
- David TS, Henriques MO, Kurz-Besson C, Nunes J, Valente J, Vaz M, Pereira JS, Siegwolf R, Chaves MM, Gazarini C, David JS (2007) Water-use strategies in two co-occurring Mediterranean evergreen oaks: surviving the summer drought. *Tree Physiol* 27:793–803
- Devitt DA, Smith SD (2002) Root-channel macropores enhance downward movement of water in the Mojave Desert ecosystem. *J Arid Environ* 50:99–108
- D'Odorico P, Caylor K, Okin GS, Scanlon TM (2007) On soil moisture-vegetation feedbacks and their possible effects on the dynamics of dryland ecosystems. *J Geophys Res* 112:G04010. doi:10.1029/2006JG000379
- Eamus D, Hutley LB, O'Grady AP (2001) Daily and seasonal patterns of carbon and water fluxes above a north Australian savanna. *Tree Physiol* 21:977–988
- Ewers BE, Mackay DS, Gower ST, Ahl DE, Burrows SN, Samanta SS (2002) Tree species effects on stand transpiration in northern Wisconsin. *Water Resour Res* 38(7):1103. doi:10.1029/2001WR000830
- Farquhar GD, Caemmerer S (1982) Modelling of photosynthetic response to environmental conditions. In: Lange OL, Nobel PS, Osmond CB, Ziegler H (eds) *Physiological Plant Ecology II*, 12/B. Springer, Berlin, pp 549–587
- Frost P, Medina E, Menaut J-C, Solbrig O, Swift M, Walker B (1986) Responses of savannas to stress and disturbance. *Biology International (I.U.B.S.)*. NTIS, 10, Paris
- Gibbens RP, Lenz JM (2001) Root systems of some Chihuahuan Desert plants. *J Arid Environ* 49:221–263
- Granier A (1987) Evaluation of transpiration in a Douglas-fir stand by means of sap flow measurements. *Tree Physiol* 3:309–320
- Hamerlynck EP, Scott RL, Moran MS, Schwander AM, Connor E, Huxman TE (2011) Inter- and under-canopy soil water, leaf-level and whole-plant gas exchange dynamics of a semi-arid perennial C₄ grass. *Oecologia* 165:17–29
- Harley PC, Tenhunen JD (1991) Modeling the photosynthetic response of C₃ leaves to environmental factors. In: Boote

- KJ, Loomis RS (eds) Modeling crop photosynthesis- from biochemistry to canopy. Crop Science Society of America, Anaheim, pp 17–39
- Hudak T, Wessman CA (1998) Textural analysis of historical aerial photography to characterize woody plant encroachment in South African Savanna. *Remote Sens Environ* 66:317–330
- Hutley LB, O'Grady AP, Eamus D (2000) Evapotranspiration from Eucalypt open-forest savanna of tropical Northern Australia. *Funct Ecol* 14:183–194
- Huxman TE, Cable JM, Ignace DD, Eilts JA, English NB, Weltzin J, Williams DG (2004) Response of net ecosystem gas exchange to a simulated precipitation pulse in a semi-arid grassland: the role of native versus non-native grasses and soil texture. *Oecologia* 141:295–305
- Jenerette GD, Scott RL, Huxman TE (2008) Whole ecosystem metabolic pulses following precipitation events. *Funct Ecol* 22:924–930
- K'Otuto GO, Otieno DO, Seo B, Ogindo HO, Onyango JC (2013) Carbon dioxide exchange and biomass productivity of the herbaceous vegetation of a managed tropical humid savanna ecosystem in western Kenya. *J Plant Ecol* 6:286–297
- Kutsch WL, Hanan N, Scholes RJ, McHugh I, Kubheka W, Eckhardt H, Williams C (2008) Response of carbon fluxes to water relations in a savanna ecosystem in South Africa. *Biogeosciences* 5:2197–2235
- Le Roux X, Bariac T, Mariotti A (1995) Spatial partitioning of the soil water resource between grass and shrub components in a West African humid savanna. *Oecologia* 104:147–155
- Maitima JM, Olson JM, Mugatha SM, Mugisha S, Mutie IT (2010) Land use changes, impacts and options for sustaining productivity and livelihoods in the basin of lake Victoria. *J Sustain Dev Afr* 12:189–206
- Merbold L, Ardo J, Arneeth A, Scholes RJ et al (2009) Precipitation as driver of carbon fluxes in 11 African ecosystems. *Biogeosciences* 6:1027–1041
- Midgley GF, Thuiller W (2010) Potential responses of terrestrial biodiversity in Southern Africa to anthropogenic climate change. *Reg Environ Change* 11:127–135
- Miranda AC, Miranda HS, Lloyd J et al (1997) Fluxes of carbon, water and energy over Brazilian cerrado, an analysis using eddy covariance and stable isotopes. *Plant Cell Environ* 20:315–328
- Mordelet R, Abbadie L, Menaut J-C (1993) Effects of tree clumps on soil characteristics in a humid savanna of West Africa (Lamto, C6te d'Ivoire). *Plant Soil* 153:103–111
- Myers BA, Duff GA, Eamus D, Fordyce IR, O'Grady A, Williams RJ (1997) Seasonal variation in water relations of trees of differing leaf phenology in a wet-dry tropical savanna near Darwin, northern, Australia. *Aust J Bot* 45:225–240
- Noy-Meir I (1982) Stability of plant-herbivore models and possible applications to savanna. In: Huntley BJ, Walker BH (eds) *Ecology of tropical savannas*. Springer, Berlin, pp 591–609
- O'Grady AP, Eamus D, Hutley LB (1999) Transpiration increases during the dry season: patterns of tree water use in eucalypt open-forests of northern Australia. *Tree Physiol* 19:591–597
- Otieno DO, Schmidt MWT, Kurz-Besson C, Lobo Do Vale R, Pereira JS, Tenhunen JD (2007) Regulation of transpirational water loss in *Quercus suber* trees in a Mediterranean-type ecosystem. *Tree Physiol* 27:1179–1187
- Otieno DO, Wartinger M, Nishiwaki A, Hussain MZ, Muhr J, Borken W, Lischeid G (2009) Responses of CO₂ exchange and primary production of the ecosystem components to environmental changes in a mountain peatland. *Ecosystems* 12:590–603
- Otieno DO, Li Y-L, Oua Y-X, Chenga J, Liua S, Tanga X, Zhanga Q, Jung E, Zhanga D, Tenhunen J (2014) Stand characteristics and water use at two elevations in a subtropical evergreen forest in southern China. *Agric For Meteorol* 194:155–166
- Owen K, Tenhunen J, Reischstein M, Wang Q, Falge E, Gayer R et al (2007) Comparison of seasonal changes in CO₂ exchange capacity of ecosystems distributed along a north-south European transect under non water stressed conditions. *Glob Change Biol* 13:734–760
- Roques KG, Oconnor TG, Watkinson AT (2001) Dynamics of shrub encroachment in an African savanna: relative influences of fire, herbivory, rainfall and density dependence. *J Appl Ecol* 19:268–280
- Ruidisch M, Nguyen TT, Li YL, Geyer R, Tenhunen J (2015) Estimation of annual spatial variations in forest production and crop yields at landscape scale in temperate climate regions. Special issue: long-term and interdisciplinary research on forest ecosystem functions: Challenges at Takayama site since 1993. *Ecol Res* 30:279–292
- Sankaran M, Ratnam J, Hanan NP (2004) Tree-grass coexistence in savannas revisited—insights from an examination of assumptions and mechanisms invoked in existing models. *Ecol Lett* 7:480–490
- Schaap MG, Leij FJ, van Genuchten MT (2001) ROSETTA: a computer program for estimating soil hydraulic parameters with hierarchical pedotransfer functions. *J Hydrol* 251:163–176
- Scholes RJ, Archer SR (1997) Tree-grass interactions in savannas. *Ann Rev Ecol Syst* 28:517–544
- Scholes RJ, Walker BH (1993) *The African savanna*. Synthesis of the Nylsvley study. Cambridge University Press, Cambridge
- Scott RL, Huxman TE, Williams DG, Goodrich DC (2006) Ecohydrological impacts of woody plant encroachment: seasonal patterns of water and carbon exchange within a semi-riparian environment. *Glob Change Biol* 12:311–324
- Scott RL, Huxman TE, Barron-Gafford GA, Jenerette DG, Young JM, Hamerlynck EP (2014) When vegetation change alters ecosystem water availability. *Glob Change Biol* 20:2198–2210
- Sillmann J, Kharin VV, Zwiers FW, Zhang X, Bronaugh D (2013) Climate extreme indices in the CMIP5 multi-model ensemble. Part 2: future climate projections. *J Geophys Res Atmos* 118:2473–2493
- van Genuchten MT (1980) A closed-form equation for predicting the hydraulic conductivity of unsaturated soils. *Soil Sci Soc Am J* 44:892–898
- Veenendaal EM, Kolle O, Lloyd J (2004) Seasonal variation in energy fluxes and carbon dioxide exchange for a broad-leaved semi-arid savanna (mopane woodland) in southern Africa. *Glob Change Biol* 10:318–328

- Walker BH, Noy-Meir I (1982) Aspects of the stability and resilience of savanna ecosystems. In: Huntley BJ, Walker BH (eds) Ecology of tropical savannas. Springer, Berlin, pp 556–590
- Walter H (1971) In: Burnett JH (ed) Ecology of tropical and subtropical vegetation. Oliver & Boyd, Edinburgh
- Wang L, D'Odorico P, Ringrose S, Coetzee S, Macko SA (2007) Biogeochemistry of Kalahari sands. *J Arid Environ* 71:259–279
- Weltzin JF, Coughenour MB (1990) Savanna tree influence on understory vegetation and soil nutrients in northwestern Kenya. *J Veg Sci* 1:325–334
- Williams CA, Albertson JD (2004) Soil moisture controls on canopy-scale water and carbon fluxes in an African savanna. *Water Resour Res* 40:W09302. doi:[10.1029/2004WR003208](https://doi.org/10.1029/2004WR003208)
- Williams CA, Hanan NP, Neff JC, Scholes RJ, Berry JA, Denning AS, Baker DF (2007) Africa and the global carbon cycle. *Carbon Balance Manag* 2:3. doi:[10.1186/1750-0680-2-3](https://doi.org/10.1186/1750-0680-2-3)
- Williams CA, Hanan N, Scholes RJ, Kutsch W (2009) Complexity in water and carbon dioxide fluxes following rain pulses in an African savanna. *Oecologia* 161:469–480
- Wong SC, Cowan IR, Farquhar GD (1979) Stomatal conductance correlates with photosynthetic capacity. *Nature* 282:424–426
- Xu L, Baldocchi DD (2003) Seasonal trends in photosynthetic parameters and stomatal conductance of blue oak (*Quercus douglasii*) under prolonged summer drought and high temperature. *Tree Physiol* 23:865–877